INSTITUTE OF PHYSICS PUBLISHING JOURNAL OF PHYSICS B: ATOMIC, MOLECULAR AND OPTICAL PHYSICS

J. Phys. B: At. Mol. Opt. Phys. **34** (2001) 1185–1199 www.iop.org/Journals/jb PII: S0953-4075(01)18000-4

Integral cross sections for electron impact excitation of electronic states of N_2

L Campbell[1], M J Brunger[1], A M Nolan[1], L J Kelly[2], A B Wedding[3], J Harrison[1], P J O Teubner[1], D C Cartwright[4] and B McLaughlin[5]

[1] School of Chemistry, Physics and Earth Sciences, The Flinders University of South Australia, GPO Box 2100, Adelaide, SA 5001, Australia
[2] Maritime Operations Division, Defence Science and Technology Organisation, PO Box 1500, Salisbury, SA 5108, Australia
[3] School of Electrical and Information Engineering, University of South Australia, Mawson Lakes, SA 5095, Australia
[4] Theoretical Divisions, Los Alamos National Laboratory, Los Alamos NM 87545, USA
[5] Department of Applied Mathematics and Theoretical Physics, The Queen's University of Belfast, Belfast BT7 1NN, UK

Received 13 October 2000, in final form 29 January 2001

Abstract

We report integral cross sections (ICSs) for electron impact excitation of the $A\ ^3\Sigma_u^+$, $B\ ^3\Pi_g$, $W\ ^3\Delta_u$, $B'\ ^3\Sigma_u^-$, $a'\ ^1\Sigma_u^-$, $a\ ^1\Pi_g$, $\omega\ ^1\Delta_u$, $C\ ^3\Pi_u$, $E\ ^3\Sigma_g^+$ and $a''\ ^1\Sigma_g^+$ electronic states of N_2. The present data, for each state, were derived at five incident electron energies in the range 15–50 eV, from the earlier crossed-beam differential cross section (DCS) measurements of our group. This was facilitated by using a molecular phase shift analysis technique to extrapolate the measured DCSs to 0° and 180°, before performing the integration. A comprehensive comparison of the present ICSs with the results of earlier experimental studies, both crossed beam and electron swarm, and theoretical calculations is provided. This comparison clearly indicates that some of the previous estimates for these excited electronic-state cross sections need to be reassessed. In addition, we have used the present ICSs in a Monte Carlo simulation for modelling the behaviour of an electron swarm in the bulk of a low current N_2 discharge. The macroscopic transport parameters determined from this simulation are compared against those measured from independent swarm-based experiments and the self-consistency of our ICSs evaluated.

(Some figures in this article are in colour only in the electronic version; see `www.iop.org`)

1. Introduction

The interaction between molecular nitrogen (N_2) and electrons plays a very important role in many diverse physical phenomena in the Earth's atmosphere [1]. N_2 has also been an important species for study in many gaseous electronics experiments [2].

It is thus somewhat surprising that the available crossed-beam integral cross sections (ICS), for electron impact excitation of the ten lowest-lying excited electronic states of N_2 ($A\ ^3\Sigma_u^+$, $B\ ^3\Pi_g$, $W\ ^3\Delta_u$, $B'\ ^3\Sigma_u^-$, $a'\ ^1\Sigma_u^-$, $a\ ^1\Pi_g$, $\omega\ ^1\Delta_u$, $C\ ^3\Pi_u$, $E\ ^3\Sigma_g^+$ and $a''\ ^1\Sigma_g^+$), are still somewhat limited in their scope. Apart from the pioneering studies of Cartwright *et al* [3] that were renormalized by Trajmar *et al* [4], the remaining crossed-beam experimental studies [5–12] have been largely restricted to considering only a small subset of these excited electronic states. Specifically, the work of Finn and Doering [5] and Mason and Newell [6] concentrated on ICS for the $a\ ^1\Pi_g$ state, Brunger *et al* [7] only looked at a near-threshold ICS for the $E\ ^3\Sigma_g^+$ state, while Zubek and King [8] and Poparić *et al* [9, 10] reported ICS for the $E\ ^3\Sigma_g^+$ and $C\ ^3\Pi_u$ electronic states. An earlier optical measurement for the $B\ ^3\Pi_g$ and $C\ ^3\Pi_u$ states by Stanton and St John [11] and a metastable excitation function for the $E\ ^3\Sigma_g^+$ electronic state from Borst *et al* [12] are also noted for completeness. From a theoretical perspective we highlight the distorted-wave (DW) ICS calculation from Fliflet *et al* [13] for the $B\ ^3\Pi_g$, $C\ ^3\Pi_u$ and $E\ ^3\Sigma_g^+$ states, the *R*-matrix ICS calculation [14] for the $A\ ^3\Sigma_u^+$, $B\ ^3\Pi_g$, $W\ ^3\Delta_u$ and $B'\ ^3\Sigma_u^-$ electronic states and a quite recent finite element *Z*-matrix method result [15] for the $A\ ^3\Sigma_u^+$ state.

In addition to the restricted nature of the previous experimental and theoretical studies, as well as the fact that the agreement between these various cross sections for a given electronic state are often marginal [5–15], we also note that the crossed-beam ICS are, in general, in only fair agreement with those used in swarm studies (e.g. Boltzmann or Monte Carlo analyses) [2,16] to reproduce macroscopic transport parameters including Townsend's primary ionization coefficient (α_T), the drift velocity (W) and the transverse (D_T) and longitudinal (D_L) diffusion coefficients, both traditionally being divided by the electron mobility (μ), as functions of the reduced electric field ($\frac{E}{N}$).

Consequently we have applied a molecular phase shift analysis (MPSA) technique [17] to the earlier differential cross section (DCS) measurements from our group [18], and derived ICS at five energies (E_0) in the range 15–50 eV for electron impact excitation of the ten lowest-lying excited electronic states of N_2.

Further, these ICSs have been employed in Monte Carlo simulations of N_2 discharges for a range of reduced electric fields[6] corresponding to the availability (typically from about 100 to 600 Td) of recent experimental data [19–27] to derive values for $\frac{\alpha_T}{p_0}$, W, $\frac{D_T}{\mu}$ and $\frac{D_L}{\mu}$.

Details of our MPSA procedure and Monte Carlo simulation are provided in the next section. Following this in section 3.1 we give the present ICS and a comprehensive comparison and discussion of these data with other experimental and theory results. In section 3.2 we present the results from our Monte Carlo simulation and compare them against the available experimental transport coefficient data and the results from other simulations. Finally, some conclusions from this paper are drawn in section 4.

2. Method of analysis

2.1. Molecular phase shift analysis technique

We have in essence applied the MPSA technique of Boesten and Tanaka [17] to the DCS measurements of Brunger and Teubner [18], for each state and at every energy of that work.

[6] The reduced electric field $\frac{E}{N}$ is the ratio of the electric field strength E to the molecular density N and has units of Townsend (1 Td $\equiv 10^{-21}$ V m^2). This parameter determines the equilibrium transport behaviour in a gas discharge.

The basis of the MPSA is to write the scattering amplitude as

$$f(\theta) = \frac{1}{2ik}\sum_{\ell=0}^{L}(2\ell+1)\,(e^{2i\delta_\ell}-1)\,P_\ell\,(\cos\theta) + \frac{1}{2ik}\sum_{\ell_>=L+1}^{\ell_{max}}(2\ell_>+1)\,(e^{2i\delta_{\ell_>}}-1)\,P_{\ell_>}(\cos\theta) \tag{1}$$

with, for $\ell > L$,

$$\tan\,\delta_{\ell_>} = \frac{\alpha\pi k^2}{(2\ell_>+3)(2\ell_>+1)(2\ell_>-1)}. \tag{2}$$

The DCS then follows from the relation

$$\sigma(\theta) = |f(\theta)|^2. \tag{3}$$

Here k is the wavenumber of the free electron, $P_\ell(\cos\theta)$ are the Legendre polynomials, α is the dipole polarizability of the target (=11.744 a_0^3 [28] for N_2) and δ_ℓ are the 'phase shifts' of the partial waves. Note we have annotated 'phase shifts' because electron scattering from the linear N_2 molecule is clearly not a straightforward central potential problem. Consequently the 'phase shifts' we derive cannot directly be interpreted as corresponding to those that we are all familiar with from the central potential scattering system. Indeed the physical meaning of our derived 'phase shifts', for electronic excitation in a linear molecule, is unclear beyond that of being the free parameters in the functional form given by equations (1) and (3) and used in our fits. However the MPSA has been applied successfully to many molecular systems by both the Sophia and Kaiserslautern groups. The utility of this approach to molecular systems would appear to originate from the following two observations. Firstly the crossed beam experiments average over all orientations of the N_2 molecule which results in the fact that any molecular axis orientation dependence is lost in the experimental data. Hence the use of a spherically symmetric concept in the data analysis. Secondly when one looks at the total electron density of the respective molecular systems studied using the MPSA technique, then to a very good approximation they appear to mimic a central potential problem. The quantity $\tan\delta_{\ell_>}$ summarizes the contributions of the higher partial waves ($\ell > L$ up to some ℓ_{max}) by using the Born series result.

In the MPSA procedure equations (1)–(3) are fitted to the experimental DCS data by a least-squares algorithm (χ^2-minimization) [29]. The phase shifts for $\ell = 0$ to L are treated as the free parameters to be determined in the fit. In this paper $L = 7$ was typically sufficient to give a good fit to the DCS. Note that the size factor $N(k)$, often employed in equation (1) as an additional parameter in the fit, by Boesten and Tanaka [17] is not utilized in our application. Similarly the inelasticity parameter (β_ℓ), for inelastic phase-shift fitting, of Boesten and Tanaka [17] is effectively fixed here at a value of 1 for all $\ell \leqslant L$. This is equivalent to assuming the phase shifts are real, whereas in general they are in fact complex. Nonetheless, even with these additional approximations, the resultant fit removes a lot of the subjectivity in the extrapolation of the measured DCS to 0° and 180°. Note that our approximation of setting $\beta_\ell = 1$ was tested thoroughly against available convergent close coupling (CCC) DCS results from Bray and colleagues, for the $1\,^1S$, $2\,^1S$ and $2\,^3P$ states of helium at energies in the range 1.5–50 eV. In these tests the respective CCC DCS, from $\theta_e = 10°$–90° in 10° increments, were fitted using our procedure and the corresponding ICS determined. In all cases the derived ICS from our analysis were in good agreement with those calculated directly from the CCC to better than 10%.

We have further developed the MPSA so that the present version of the program allows realistic errors to be assigned to the derived ICS by testing the sensitivity of the value of the ICS to the form of the DCS, in the experimentally inaccessible angular regions. This is achieved by specifying a range of possible DCS values at, say, $\theta_e = 140°$ and 180° and then tracking

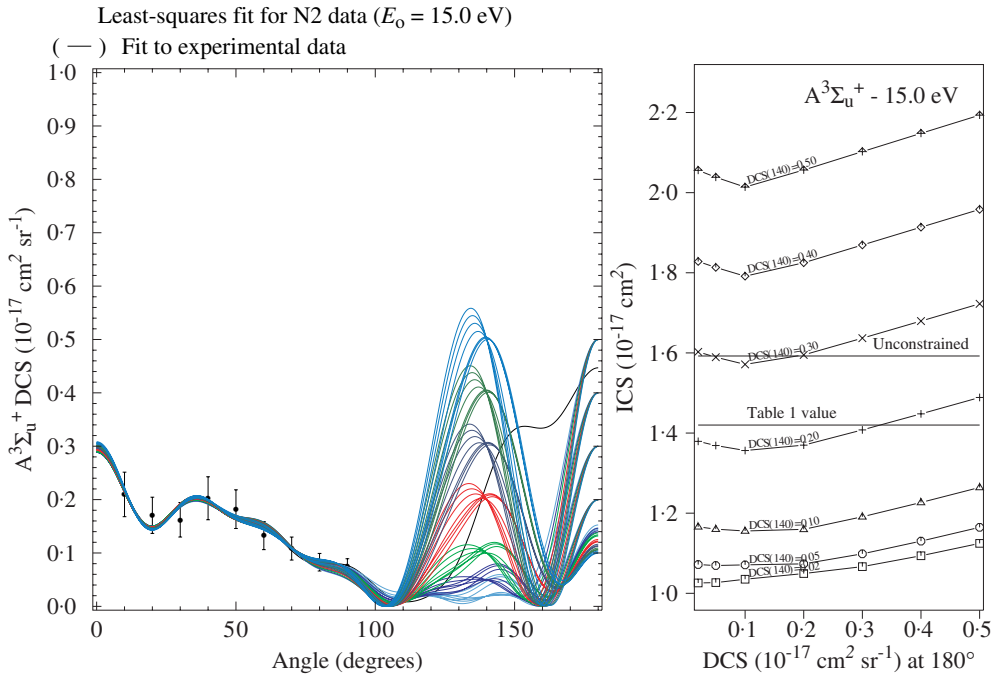

Figure 1. Results of the unconstrained and sensitivity MPSA fits (——) to the 15 eV $A\,^3\Sigma_u^+$ DCS of Brunger and Teubner [18] (left panel), and the corresponding results for the variation of the determined ICS with choice of $\theta_e = 140^\circ$ and 180° sensitivity DCS values (right panel). All units are in 10^{-17} cm^2 for the ICS and 10^{-17} cm^2 sr^{-1} for the DCS.

how the fit, and thus ultimately the value of the ICS, varies with these DCSs. A representative example for the result of this process, for the $A\,^3\Sigma_u^+$ electronic state at 15 eV, is given in figure 1. Note that the choice of the sensitivity test range values was often, initially, aided by the results of available calculations [13,14] or other experimental measurements [4,8]. If the range chosen was too large, about the optimal values indicated by theory or other experiment, then the fits were typically found to oscillate at backward angles. These unphysical oscillations are also illustrated in figure 1. We note that these cases were excluded when determining our values for the relevant ICS and the error on that ICS. Consequently, in some sense, the fits themselves placed restrictions on the range of sensitivity values that could be employed. Further note that, as expected, when the measured DCS was strongly peaked in the forward direction [18] the derived ICS did not exhibit a pronounced dependence on the choice for the sensitivity test DCS values.

Having used the MPSA to obtain the angular extrapolation to 0° and 180°, the integral

$$I_i(E_0) = \int_0^\pi (\mathrm{DCS}(E_0,\theta))_i \ \sin\theta \,\mathrm{d}\theta \tag{4}$$

was evaluated at each E_0 for each electronic-state excitation process i. The ICS_i for excitation to state i was then evaluated in the usual fashion using

$$\mathrm{ICS}_i(E_0) = 2\pi \ I_i(E_0). \tag{5}$$

The values for the respective excited electronic-state ICSs, as listed in table 1, were essentially found from the average of the unconstrained and allowed sensitivity test ICS values, as determined from the MPSA fit and Simpson's rule. The errors on the ICS in table 1 are formed

from the standard deviation in the above calculation of the respective average ICS values, and an uncertainty due to the error on the corresponding DCS measurements of Brunger and Teubner [18].

2.2. Monte Carlo simulation

The present ICSs have been used to complement a set of cross sections employed previously, in simulation studies, by Nolan [21] and Kelly [27]. The prior data were compiled by Kelly [27] using the cross sections of Ohmori *et al* [2] as a base and describe channels for elastic, ionization and dissociation collisions, along with ten ground state vibrational channels and twenty other inelastic channels. The cross section data are represented with an energy resolution of 0.05 eV. In compiling these data Kelly extended the maximum energy from 50 to 250 eV using an energy dependence appropriate to the excitation type; for example the singlet state cross sections were extrapolated with either a (E_0^{-1}) or $(E_0^{-1} \ln E_0)$ dependence, as suggested by Chung and Lin [30]. In addition, excitation to the $B\ ^2\Sigma_u^+$ state, which had previously been included as part of the total ionization cross section, was made a separate channel using the data of Borst and Zipf [31]. Note that the data of Kelly do not include cross sections for excitation of the higher lying states of N_2^+, being intended for the simulation of low to moderate reduced electric fields.

For the present Monte Carlo simulation study our ten electronic-state ICSs replaced those used in the original data base by Kelly and Nolan. To incorporate the present ICSs into this data set [21, 27] we used a simple scaling technique. The Kelly data were scaled so that her cross section values aligned exactly with our ICSs at the measurement energies (15, 17.5 eV etc). In between these energies the multiplicative scaling factor was determined by a linear extrapolation. The multiplicative scaling factor at process onset and end was unity.

This modified (compared to [21, 27]) cross section set was then used in a low current Townsend discharge simulation for reduced electric fields in the range 100–1000 Td. The gas was simulated as stationary with pressure $p_0 = 1$ Torr. Electron–gas scattering events were modelled as isotropic. Electrons were injected from a point source and transport simulated for a fixed flight time in the uniform electric field of a boundary free region. The low current density in the drift region remote from the source allows the equilibrium electron transport to be simulated by the ensemble average of a large number of separately simulated electrons and their ionization progeny. The simulations employed the null collision method developed independently by Skullerud [32] and Rees [33, 34] and popularized by Lin and Bardsley [35]. This method adds to the physical data a 'null' cross section, the magnitude of which varies such that the total collision cross section varies inversely with the square root of energy, providing for a constant mean free time between collisions and thereby simplifying the simulation process.

Typically 300 000 electrons were simulated for a 500 ns flight time during which their phase coordinates were logged at 0.5 ns intervals. In order to provide a swarm as close to equilibrium as possible, the first electron was injected with 0.1 eV energy and subsequent electrons were injected with the final energy of the previously simulated electron, but with randomized direction. To provide adequate statistics the simulations were run ten times at each value of the reduced electric field with independent seeding of the RANMAR [36] random number generator. The transport parameters for the swarm were calculated post-simulation by time derivatives of moments in configuration space [37]. For each simulation the transport parameters were averaged over the last 175 ns of the flight. Ensemble averages were then made of the transport parameters calculated from the individual simulations, with the standard deviation of the ensemble used to provide an estimate of uncertainty in the mean. Due to the method of calculation the uncertainty in the drift velocity was lower than that of the electron diffusion coefficients.

Table 1. ICSs ($\times 10^{-17}$ cm^2) for the electron impact excitation of the ten lowest-lying excited electronic states of N_2. The corresponding absolute errors in these ICS are also shown.

State	Energy (eV)	Integral cross section (10^{-17} cm^2)
$A\,^3\Sigma_u^+$	15.0	1.42 ± 0.50
	17.5	1.60 ± 0.45
	20.0	1.11 ± 0.40
	30.0	0.78 ± 0.30
	50.0	0.55 ± 0.22
$B\,^3\Pi_g$	15.0	4.51 ± 1.53
	17.5	2.82 ± 0.89
	20.0	1.34 ± 0.55
	30.0	0.87 ± 0.25
	50.0	0.49 ± 0.15
$W\,^3\Delta_u$	15.0	1.92 ± 0.50
	17.5	2.11 ± 0.53
	20.0	1.08 ± 0.34
	30.0	0.60 ± 0.21
	50.0	0.20 ± 0.08
$B'\,^3\Sigma_u^-$	15.0	2.04 ± 0.82
	17.5	1.24 ± 0.43
	20.0	0.71 ± 0.18
	30.0	0.38 ± 0.14
	50.0	0.27 ± 0.08
$a'\,^1\Sigma_u^-$	15.0	1.23 ± 0.32
	17.5	0.42 ± 0.18
	20.0	0.34 ± 0.12
	30.0	0.18 ± 0.07
	50.0	0.12 ± 0.06
$a\,^1\Pi_g$	15.0	4.32 ± 1.47
	17.5	4.69 ± 1.54
	20.0	2.66 ± 0.80
	30.0	2.25 ± 0.66
	50.0	1.32 ± 0.36
$\omega\,^1\Delta_u$	15.0	0.78 ± 0.23
	17.5	0.57 ± 0.22
	20.0	0.38 ± 0.20
	30.0	0.108 ± 0.038
	50.0	0.052 ± 0.018
$C\,^3\Pi_u$	15.0	5.18 ± 1.35
	17.5	3.04 ± 0.88
	20.0	1.61 ± 0.48
	30.0	0.95 ± 0.30
	50.0	0.34 ± 0.12
$E\,^3\Sigma_g^+$	15.0	0.031 ± 0.012
	17.5	0.057 ± 0.022
	20.0	0.170 ± 0.059
	30.0	0.110 ± 0.041
	50.0	0.0198 ± 0.0099
$a''\,^1\Sigma_g^+$	15.0	0.42 ± 0.17
	17.5	0.52 ± 0.19
	20.0	0.63 ± 0.23
	30.0	0.31 ± 0.16
	50.0	0.17 ± 0.05

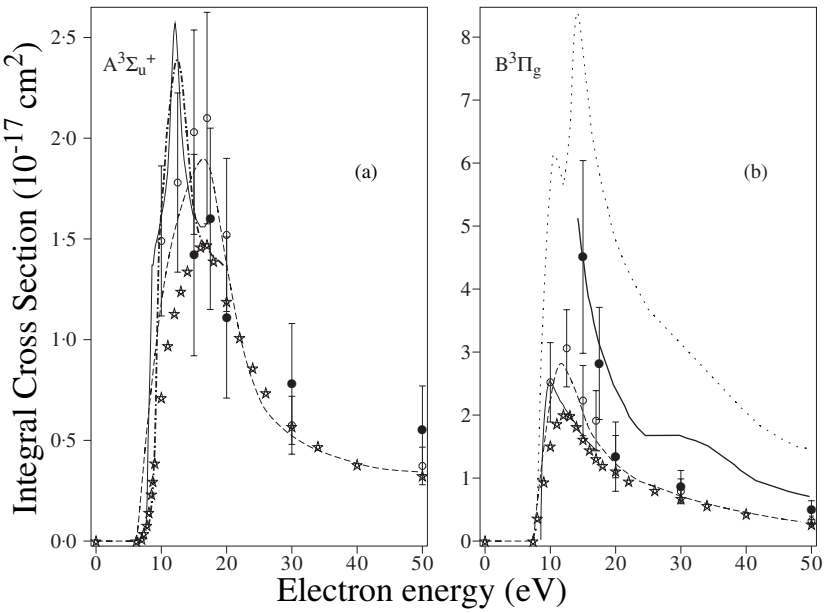

Figure 2. ICSs (10^{-17} cm^2) for the electron impact excitation of the (*a*) A $^3\Sigma_u^+$ and (*b*) B $^3\Pi_g$ electronic states. The present data (●) are compared against the earlier crossed-beam results from Trajmar *et al* [4] (○), the optical measurement of Stanton and St John [11] (- - - -), the swarm-derived results from Ohmori *et al* [2] (— — —) and Phelps and Pitchford [16] (⋆) and the theoretical calculations from Gillan *et al* [14] (——), Huo and Dateo [15] (- – - —) and Fliflet *et al* [13] (———).

To assist the tractability of the simulation when ionization growth became significant, a method of density scaling was used to maintain the swarm numbers approximately constant, as recommended by Li *et al* [38]. In our method the electrons were culled with a fixed probability prior to each simulated collision (both null and real). The culling probability was determined by trial and error for each value of the reduced electric field, ranging from 1.7% at 400 Td to 20.5% at 1000 Td. The simulated collision times were energy independent due to the use of the null collision method and so this culling procedure had no effect on the simulated electron energy distribution. With the density scaling process in place, it was not possible to use a simple calculation of the growth coefficient of the swarm to determine Townsend's first coefficient of ionization. Instead this parameter was determined by the product of the equilibrium energy distribution and the energy-dependent ionization frequency, integrated over all energies [39].

3. Results and discussion

3.1. Integral cross sections

In table 1 we list the current ICS, at $E_0 = 15$, 17.5, 20, 30 and 50 eV, for the electron impact excitation of the respective A $^3\Sigma_u^+$, B $^3\Pi_g$, W $^3\Delta_u$, B′ $^3\Sigma_u^-$, a′ $^1\Sigma_u^-$, a $^1\Pi_g$, ω $^1\Delta_u$, C $^3\Pi_u$, E $^3\Sigma_g^+$ and a″ $^1\Sigma_g^+$ electronic states of N_2. Also included in this table are the errors on these ICS. In figures 2–4 the present ICS are plotted against the available theory [13–15] and previous experimental determinations [2–12, 16].

Of the ten electronic states that we have considered in this paper, it would appear from figures 2–4 that, to within the uncertainties on the respective data sets, our ICSs for the E $^3\Sigma_g^+$

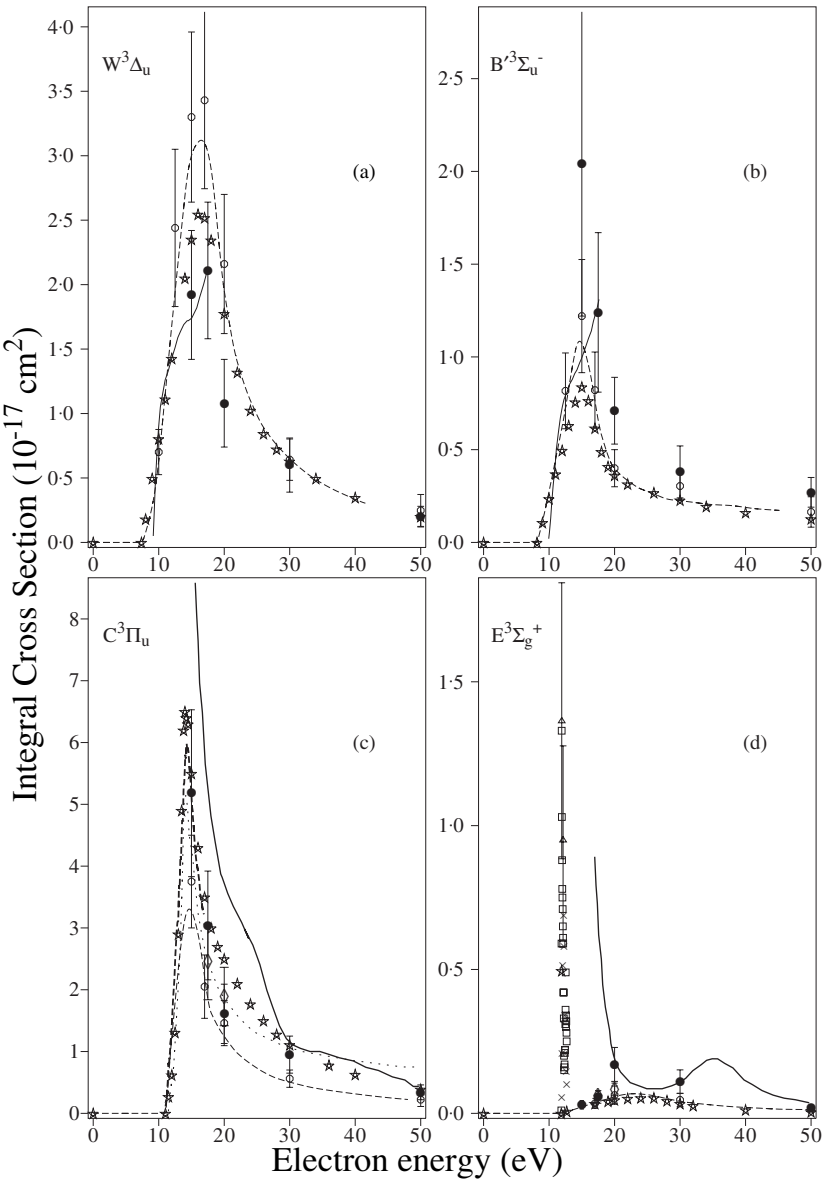

Figure 3. ICSs (10^{-17} cm^2) for the electron impact excitation of the (*a*) W $^3\Delta_u$, (*b*) B$'$ $^3\Sigma_u^-$, (*c*) C $^3\Pi_u$ and (*d*) E $^3\Sigma_g^+$ electronic states. The present data (●) are compared against the earlier crossed beam results from Trajmar *et al* [4] (○), Zubek and King [8] (◇), Poparić *et al* [10] (— — —) and Poparić *et al* [9] (△), the optical measurement of Stanton and St John [11] (- - - -), the metastable excitation function measurements of Brunger *et al* [7] (△) and Borst *et al* [12] (×), the swarm-derived results from Ohmori *et al* [2] (— — —) and Phelps and Pitchford [16] (⋆) and the theoretical calculations from Gillan *et al* [14] (——) and Fliflet *et al* [13] (———).

(figure 3(*d*)), a$'$ $^1\Sigma_u^-$ (figure 4(*a*)), ω $^1\Delta_u$ (figure 4(*c*)) and a$''$ $^1\Sigma_g^+$ states (figure 4(*d*)) are in good agreement with the earlier work of Trajmar *et al* [4]. This comment applies for those ICSs across the entire range of common energies and so it effectively defines an optimum crossed-beam ICS result for each of these states. In addition, concentrating on figure 3(*d*), we

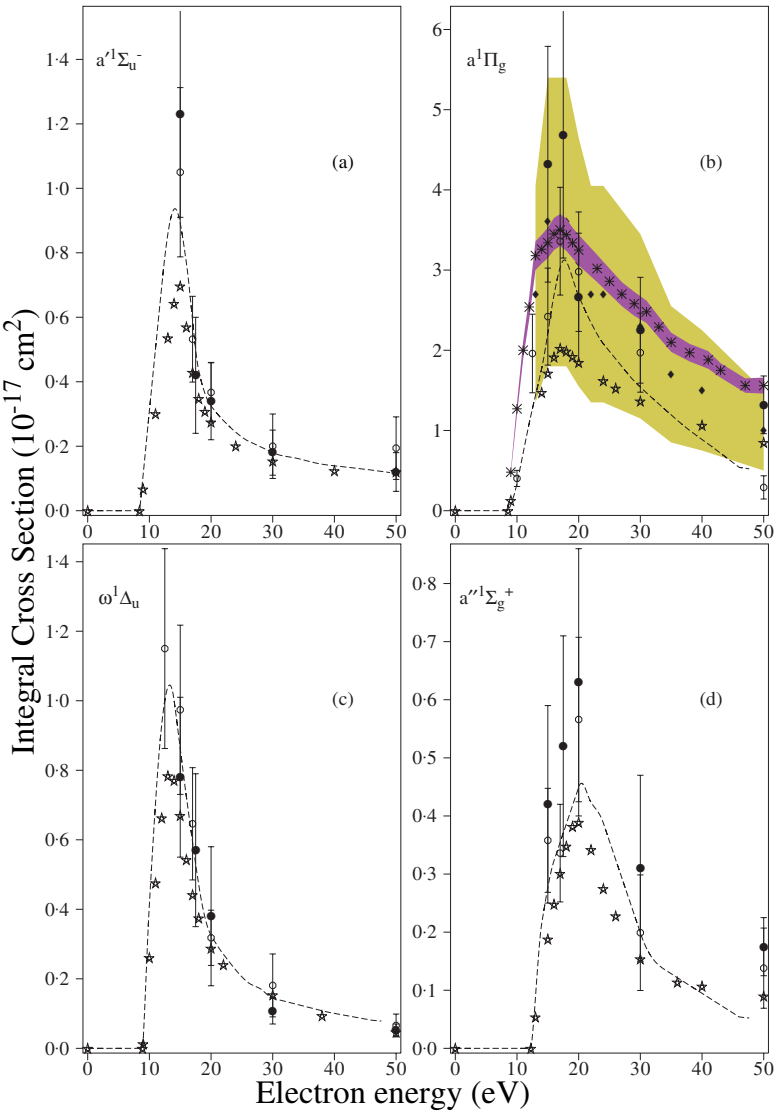

Figure 4. ICSs (10^{-17} cm^2) for the electron impact excitation of the (*a*) a′ $^1\Sigma_u^-$, (*b*) a $^1\Pi_g$, (*c*) ω $^1\Delta_u$ and (*d*) a″ $^1\Sigma_g^+$ electronic states. The present data (●) are compared against the earlier crossed beam results from Trajmar *et al* [4] (○), Finn and Doering [5] (◇) and Mason and Newell [6] (∗) and the swarm-derived results from Ohmori *et al* [2] (— — —) and Phelps and Pitchford [16] (⋆). Note that the shaded regions in (*b*) represent the respective uncertainties on the measurements of Finn and Doering and Mason and Newell.

observe that for the E $^3\Sigma_g^+$ state the measurements of Zubek and King [8] are in fair accord with both the present ICS and those of Trajmar *et al* [4]. Similarly it is apparent that the recent near-threshold experiment for the E $^3\Sigma_g^+$ electronic state of Poparić *et al* [9] confirms the position and magnitude of the resonance enhanced ICS that was originally observed by Brunger *et al* [7]. It is interesting to note that neither of the swarm-derived cross sections [2,16] utilize this near-threshold behaviour of the E $^3\Sigma_g^+$ state ICS. Finally we highlight the good level

of agreement between the present ICS and the DW calculation of Fliflet *et al* [13], for the E $^3\Sigma_g^+$ state at $E_0 \geqslant 20$ eV (figure 3(*d*)).

It is also clear from figures 2–4 that there is quite a good level of agreement between the present ICS and those of Trajmar *et al* [4] for energies $E_0 > 20$ eV, for the remaining A $^3\Sigma_u^+$, B $^3\Pi_g$, W $^3\Delta_u$, B′ $^3\Sigma_u^-$, a $^1\Pi_g$ and C $^3\Pi_u$ electronic states, thereby again effectively defining an optimum crossed-beam result for this kinematic regime. However, for $E_0 \leqslant 20$ eV the present ICSs for the A $^3\Sigma_u^+$ (figure 2(*a*)) and W $^3\Delta_u$ (figure 3(*a*)) states appear to be systematically lower in magnitude when compared to those found by Trajmar *et al* [4]. With respect to this we note that the swarm-derived ICSs of Phelps and Pitchford [16] favour the present determinations for both the A $^3\Sigma_u^+$ and W $^3\Delta_u$ states, and that both the *R*-matrix calculation [14] ICS and the finite element *Z*-matrix calculation [15] ICS also are in better agreement with the present A $^3\Sigma_u^+$ ICS than they are with the corresponding ICS of Trajmar *et al* [4]. Similarly the *R*-matrix result [14] for the W $^3\Delta_u$ state is in better agreement with our determination of the ICS than with that reported in Trajmar *et al* [4].

Considering the remaining B $^3\Pi_g$, B′ $^3\Sigma_u^-$, C $^3\Pi_u$ and a $^1\Pi_g$ states, again for $E_0 \leqslant 20$ eV, the present ICSs for the B $^3\Pi_g$ (figure 2(*b*)), B′ $^3\Sigma_u^-$ (figure 3(*b*)), C $^3\Pi_u$ (figure 3(*c*)) and a$^1\Pi_g$ (figure 4(*b*)) electronic states appear to be systematically higher in magnitude when compared to those found by Trajmar *et al* [4].

Concentrating, initially, on the B $^3\Pi_g$ state (figure 2(*b*)) we see that both the swarm-derived ICS result of Phelps and Pitchford [16] and the *R*-matrix ICS calculation of Gillan *et al* [14] underestimate the magnitude of the crossed-beam ICSs, although here they are closer in value to those of Trajmar *et al* [4]. The optical result [11] significantly overestimates the magnitude of the ICS for the B $^3\Pi_g$ state, reflecting important cascade contributions to the measured signal. Consequently this latter measurement [11] does not shed much light as to the veracity of the present ICS or those of Trajmar *et al* [4] at $E_0 \leqslant 20$ eV. On the other hand we note that the DW-theory calculation of Fliflet *et al* [13] (see figure 2(*b*)) is in good agreement with the present ICS for $E < 20$ eV, although at higher energies it tends to overestimate the magnitude of this ICS.

Considering the C $^3\Pi_u$ electronic-state ICS in more detail for $E_0 \leqslant 20$ eV, we note from figure 3(*c*) that the independent measurements of Zubek and King [8] and Poparić *et al* [10] tend to favour the present ICS over those determined by Trajmar *et al* [4]. Furthermore the swarm-derived cross section of Phelps and Pitchford [16] is also in good agreement with the present results. These results have important ramifications at the DCS level where the shapes and magnitudes of the C $^3\Pi_u$ DCS of Trajmar *et al* [4] and Brunger and Teubner [18], particularly at $E_0 \leqslant 20$ eV, are in quite poor agreement. In addition we note that while the DW calculation of Fliflet *et al* [13] is in quite good agreement with the present ICS at $E_0 = 30$ and 50 eV, at lower energies it seriously overestimates the magnitude of this ICS (figure 3(*c*)).

A similar situation to that described above is also found for the a $^1\Pi_g$ state (figure 4(*b*)), at $E_0 \leqslant 20$ eV, where the independent ICS results of Finn and Doering [5] and Mason and Newell [6] tend to be systematically larger in magnitude than those of Trajmar *et al* [4]. This observation is compatible with the present ICS results, although in this case it is also clear that all the crossed-beam data are in agreement with one another to within their respective stated uncertainties. The electron impact excitation of the a $^1\Pi_g$ state is somewhat unusual for electronic-state excitation in molecules in that there is now a quite large number of consistent independent crossed-beam measurements for it. Consequently, on the basis of these measurements, it should be possible to construct an 'optimum'or 'recommended' a $^1\Pi_g$ ICS for use by the modelling community.

Finally, figure 3(*b*) indicates that the present ICS for the B′ $^3\Sigma_u^-$ electronic-state is systematically higher in magnitude than that of Trajmar *et al* [4] for $E_0 \leqslant 20$ eV, although

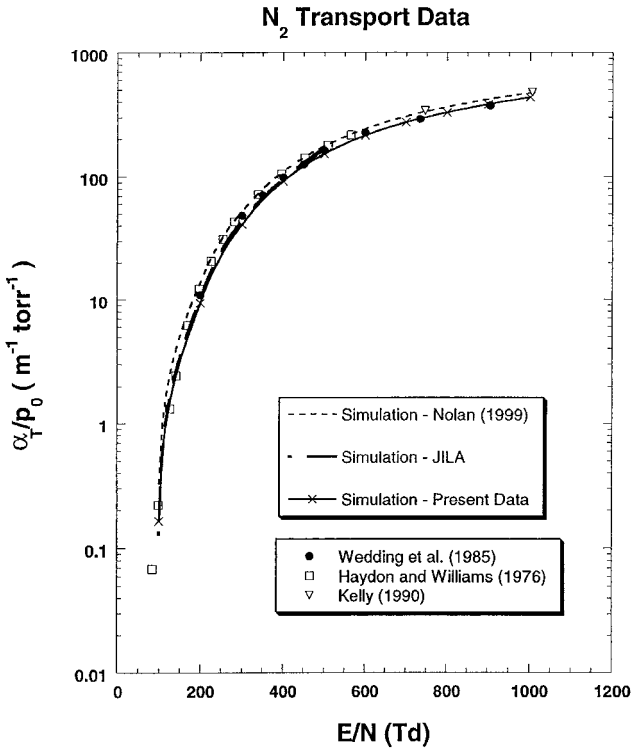

Figure 5. Townsend's primary coefficient of ionization as a function of the reduced electric field for a N_2 discharge. The experimental results of Haydon and Williams [19] (□), Wedding *et al* [20] (●) and Kelly [27] (▽) are compared against the results from the present simulation (-×-) and simulations using the JILA cross section data base [22] (— — —) and the cross section data base of Ohmori *et al* [2, 21] (- - - -).

once again there is typically overlap between these two sets of data when the respective stated uncertainties are allowed for. In this case the *R*-matrix calculation of Gillan *et al* [14] does not give any real indication as to which of the two crossed-beam experimental results might be the more reliable. This is because the *R*-matrix result favours that of Trajmar *et al* [4] at $E_0 = 15$ eV, but at $E_0 = 17.5$ eV it is in better accord with the present ICS. It should be noted that the *R*-matrix calculations of Gillan *et al* [14] were performed at one fixed internuclear geometry with no account taken of vibrational motion.

3.2. Transport coefficients

In figures 5–8 we plot the results from our Monte Carlo discharge simulations. The behaviour of the transport coefficients $\frac{\alpha_T}{p_0}$, W, $\frac{D_T}{\mu}$ and $\frac{D_L}{\mu}$ as a function of $\frac{E}{N}$ are respectively shown. Full details of our Monte Carlo simulation and the incorporation of the present ten electronic-state ICSs into the original data base of Ohmori *et al* [2] are given in section 2.2. For comparison figures 5–8 also show the results from simulations using the ICS data base of Ohmori *et al* [2, 21, 27] and the JILA ICS data base [22], as well as the appropriate available experimental transport coefficients [19, 20, 23–27].

It is clear from figure 5 that the simulated values for $\frac{\alpha_T}{p_0}$ as a function of $\frac{E}{N}$ are in good agreement with one another, largely irrespective of the cross section data base used. In addition

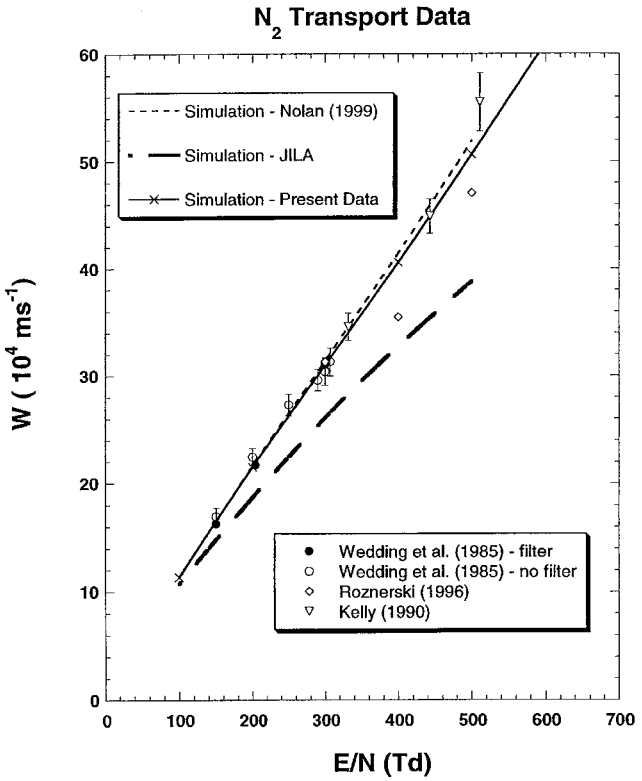

Figure 6. Drift velocity as a function of the reduced electric field for a N_2 discharge. The experimental results of Wedding *et al* [20] (●, ○), Kelly [27] (▽) and Roznerski [23] (◇) are compared against the results from the present simulation (⋇) and simulations using the JILA cross section data base [22] (— — —) and the cross section data base of Ohmori *et al* [2,21] (- - - -).

it is also apparent that they are in good accord with the experimental measurements of Haydon and Williams [19], Wedding *et al* [20] and Kelly [27], over the entire range of $\frac{E}{N}$ studied. As the ICS data bases from JILA [22], Ohmori *et al* [2] and the present are rather different (see figures 2–4) for the ten electronic states of interest to this study, the results embodied in figure 5 simply represent the lack of sensitivity of $\frac{\alpha_T}{p_0}$ to the microscopic behaviour in the swarm. A similar situation is found in figure 6 for the drift velocity as a function of $\frac{E}{N}$. In this case the result of the present simulation and that using the data base of Ohmori *et al* [2] are again in very good agreement with one another and with the experimental data of Wedding *et al* [20], Kelly [27] and, to a somewhat lesser extent, Roznerski [23]. Somewhat surprisingly, the simulation result for the drift velocity that employed the JILA data base is in very poor agreement with the other simulations and the measurements [20,23,27]. This significant discrepancy was not expected as the JILA cross section data base was constructed by Phelps and co-workers, over an extended period, to specifically reproduce macroscopic transport data at high $\frac{E}{N}$.

Figure 7 displays the behaviour of $\frac{D_T}{\mu}$ as a function of $\frac{E}{N}$. A sensitivity to the cross section data base employed in the simulation is more apparent for this transport parameter. The present Monte Carlo result reproduces the shape and magnitude of the $\frac{D_T}{\mu}$ versus $\frac{E}{N}$ behaviour, as measured by Roznerski [23], over the entire common range of $\frac{E}{N}$. It is certainly superior, in reproducing this measurement [23], to both the other simulations when the JILA and Ohmori

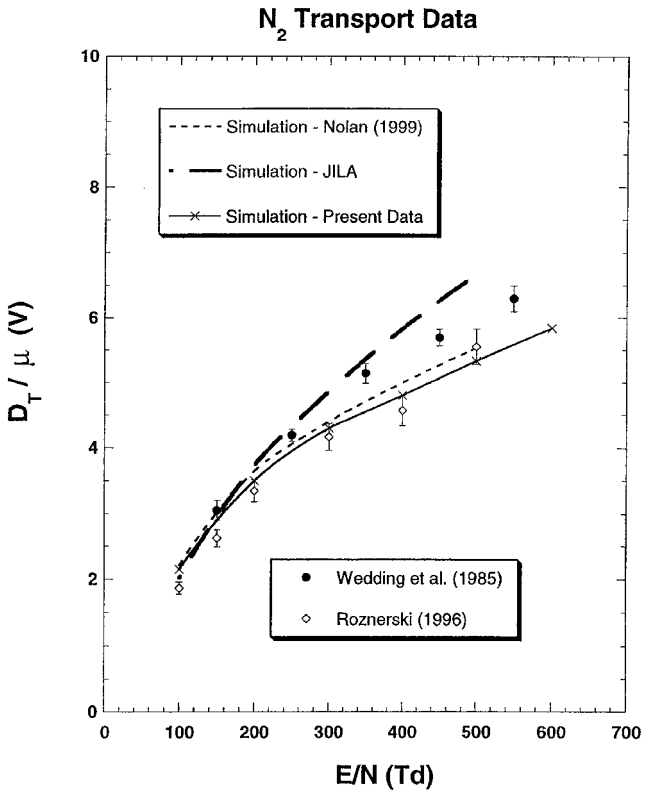

Figure 7. Ratio of the transverse diffusion coefficient to the electron mobility as a function of the reduced electric field for a N_2 discharge. The experimental results of Wedding *et al* [20] (●) and Roznerski [23] (◇) are compared against the results from the present simulation (–×–) and simulations using the JILA cross section data base [22] (— — —) and the cross section data base of Ohmori *et al* [2, 21] (- - - -).

et al data bases are used. The argument here is, however, clouded by the fact that the two available measurements for $\frac{D_T}{\mu}$ by Wedding *et al* and Roznerski are in quite poor agreement, the results of Wedding *et al* being systematically higher in magnitude than those of Roznerski. In addition, an earlier measurement for $\frac{D_T}{\mu}$ by Roznerski and Leja [40] was in good accord with that from Wedding *et al*, although Roznerski's [23] later measurements clearly supersede the earlier study. Finally, in figure 8, we consider the result of our Monte Carlo analysis for the behaviour of $\frac{D_L}{\mu}$ as a function of $\frac{E}{N}$. The first point we note about figure 8 is that $\frac{D_L}{\mu}$ is the most sensitive transport coefficient in terms of the response to the cross section data base used in the simulation. There is a clear difference in the observed behaviour of $\frac{D_L}{\mu}$ between our result and that of Nolan [21], who employed the ICSs of Ohmori *et al*. The present simulation apparently does a better job in reproducing the shape and magnitude of the most recent experimental $\frac{D_L}{\mu}$ measurements [20, 23, 27], compared to that found by Nolan. Indeed we highlight the very good agreement between the present simulation and the data of Wedding *et al* and Kelly [27] over the entire common range of $\frac{E}{N}$.

Summarizing, figures 5–8 have presented us with strong evidence that the macroscopic transport parameters are sensitive to the choice of cross section data base employed in the simulation, although some of the transport coefficients are more sensitive than others. This

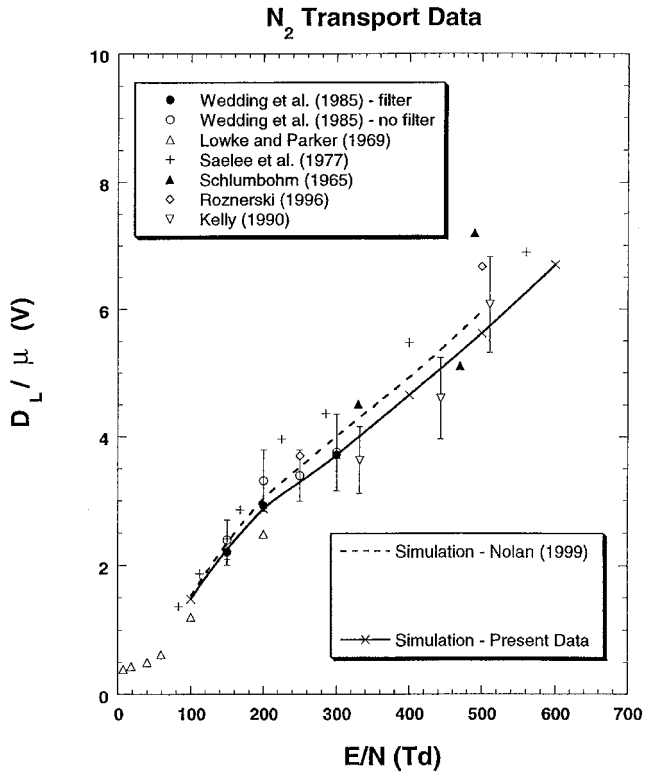

Figure 8. Ratio of the longitudinal diffusion coefficient to the electron mobility as a function of the reduced electric field for a N_2 discharge. The experimental results of Wedding *et al* [20] (●) and (○), Lowke and Parker [24] (△), Saelee *et al* [26] (+), Schlumbohm [25] (△), Kelly [27] (▽) and Roznerski [23] (◇) are compared against the results from the present simulation (-×-) and simulations using the cross section data base of Ohmori *et al* [2, 21] (- - - -).

result means that the self-consistency of a given cross section data base can be evaluated against measured transport coefficients in the range of $\frac{E}{N}$ we have studied. In particular we have found that our cross section data base (the present ten electronic-state ICS plus 23 others from Ohmori *et al* [2]), when applied in a Monte Carlo simulation of a N_2 discharge, generally reproduces the experimentally measured swarm data to a good degree of accuracy.

4. Conclusions

We have reported ICSs for the electron impact excitation of the $A\,^3\Sigma_u^+$, $B\,^3\Pi_g$, $W\,^3\Delta_u$, $B'\,^3\Sigma_u^-$, $a'\,^1\Sigma_u^-$, $a\,^1\Pi_g$, $\omega\,^1\Delta_u$, $C\,^3\Pi_u$, $E\,^3\Sigma_g^+$ and $a''\,^1\Sigma_g^+$ electronic states of N_2. The incident electron energies were 15, 17.5, 20, 30 and 50 eV in the current study. While the present investigation has confirmed an important subset of the earlier JPL ICSs [4], it has also highlighted some significant and important discrepancies between our results and the data of Trajmar *et al* [4]. Furthermore, we note that where other, relatively recent and independent, crossed-beam ICSs for electronic-state excitation in N_2 are available that they are generally in somewhat better agreement with the present ICS than those of Trajmar *et al*.

The present ICSs were incorporated into the data base of Ohmori *et al* [2] and a low current discharge simulation performed for 100 Td $\leqslant \frac{E}{N} \leqslant$ 1000 Td. Values of $\frac{\alpha_T}{p_0}$, W, $\frac{D_T}{\mu}$ and $\frac{D_L}{\mu}$ were

derived and compared to those determined by experiment. This comparison highlighted the sensitivity of the classical transport coefficients to the quantum mechanical cross sections. The present Monte Carlo transport coefficients were, in general, in quite good agreement with those measured by independent experiment [19–27]. For the $\frac{E}{N}$ range considered this demonstrates the self-consistent nature of the present ICS measurements.

Acknowledgments

This work was supported, in part, by grants from the Australian Research Council and National Science Foundation (USA).

References

[1] Cartwright D C 1978 *J. Geophys. Res.* **83** 517
[2] Ohmori Y, Shimozuma M and Tagashira H 1988 *J. Phys. D: Appl. Phys.* **21** 724
[3] Cartwright D C, Trajmar S, Chutjian A and Williams W 1977 *Phys. Rev.* A **16** 1041
[4] Trajmar S, Register D F and Chutjian A 1983 *Phys. Rev.* **97** 219
[5] Finn T G and Doering J P 1976 *J. Chem. Phys.* **64** 4490
[6] Mason N J and Newell W R 1987 *J. Phys. B: At. Mol. Phys.* **20** 3913
[7] Brunger M J, Teubner P J O and Buckman S J 1988 *Phys. Rev.* A **37** 3570
[8] Zubek M and King G C 1994 *J. Phys. B: At. Mol. Opt. Phys.* **27** 2613
[9] Poparić G, Vićić M and Belić D S 1999 *Phys. Rev.* A **60** 4542
[10] Poparić G, Vićić M and Belić D S 1999 *Chem. Phys.* **240** 283
[11] Stanton P N and St John R M 1969 *J. Opt. Soc. Am.* **59** 252
[12] Borst W L, Wells W C and Zipf E 1972 *Phys. Rev.* A **5** 1744
[13] Fliflet A W, McKoy V and Rescigno T N 1979 *J. Phys. B: At. Mol. Phys.* **19** 3281
[14] Gillan C J, Tennyson J, McLaughlin B M and Burke P G 1996 *J. Phys. B: At. Mol. Opt. Phys.* **29** 1531
[15] Huo W M and Dateo C E 1999 *Proc. 21st Int. Conf. on the Physics of Electronic and Atomic Collisions (Sendai, Japan)* ed Y Itikawa, K Okuno, H Tanaka, A Yagishita and M Matsuzawa p 294
[16] Phelps A V and Pitchford L C 1985 *Phys. Rev.* A **31** 2932
[17] Boesten L and Tanaka H 1991 *J. Phys. B: At. Mol. Opt. Phys.* **24** 821
[18] Brunger M J and Teubner P J O 1990 *Phys. Rev.* A **41** 1413
[19] Haydon S C and Williams O M 1976 *J. Phys. D: Appl. Phys.* **9** 523
[20] Wedding A B, Blevin H A and Fletcher J 1985 *J. Phys. D: Appl. Phys.* **18** 2361
[21] Nolan A M 2000 *PhD Thesis* University of South Australia, unpublished
[22] httpf//jilawww.colorado.edu/www/research/colldata.html
[23] Roznerski W 1996 *J. Phys. D: Appl. Phys.* **29** 614
[24] Lowke J J and Parker J H 1969 *Phys. Rev.* **181** 302
[25] Schlumbohm H 1965 *Z. Phys.* **184** 492
[26] Saelee H T, Lucas J and Limbeek J W 1977 *Solid-State Electron. Devices* **1** 111
[27] Kelly L J 1990 *PhD Thesis* Flinders University of South Australia, unpublished
[28] Newell A C and Baird R C 1965 *J. Appl. Phys.* **36** 3751
[29] Bevington P R and Robinson D K 1990 *Data Reduction and Error Analysis for the Physical Sciences* (New York: McGraw-Hill)
[30] Chung S and Lin C C 1972 *Phys. Rev.* A **6** 988
[31] Borst W L and Zipf E C 1970 *Phys. Rev.* A **1** 834
[32] Skullerud H R 1968 *Br. J. Appl. Phys.* (*J. Phys. D: Appl. Phys.*) **2** 1567
[33] Rees H D 1968 *Phys. Lett.* A **26** 416
[34] Rees H D 1969 *J. Phys. Chem. Solids* **30** 643
[35] Lin S L and Bardsley J N 1978 *Comput. Phys. Commun.* **15** 161
[36] James F 1990 *Rep. Prog. Phys.* **43** 1145
[37] Kumar K, Skullerud H R and Robson R E 1980 *Aust. J. Phys.* **33** 343
[38] Li Y M, Pitchford L C and Moratz T J 1989 *Appl. Phys. Lett.* **54** 1403
[39] Nolan A M, Brennan M J, Ness K F and Wedding A B 1997 *J. Phys. D: Appl. Phys.* **30** 2865
[40] Roznerski W and Leja K 1980 *J. Phys. D: Appl. Phys.* **13** L181